Smart Grid and Renewable Energy, 2024, 15, 123-138
https://www.scirp.org/journal/sgre
ISSN Online: 2151-4844
ISSN Print: 2151-481X

Design of a Three-Phase Grid Connector System Using Power Transfer from Park's Transformation

Birtukan Yenealem[1], Elias Mamushet[2]

[1]Department of Metallic Minerals Research and Development, Minerals Industry Development Institute, Ministry of Mines, Addis Ababa, Ethiopia
[2]Department of Mineral Processing Engineering, Addis Ababa Institute of Technology, Addis Ababa, Ethiopia
Email: birtyt@gmail.com, Eliasmamushet21@gmail.com

How to cite this paper: Yenealem, B. and Mamushet, E. (2024) Design of a Three-Phase Grid Connector System Using Power Transfer from Park's Transformation. *Smart Grid and Renewable Energy*, **15**, 123-138.
https://doi.org/10.4236/sgre.2024.155008

Received: May 2, 2024
Accepted: May 28, 2024
Published: May 31, 2024

Abstract

Instabilities in grid-connected inverters can arise from a number of sources, including mismatched parameters, grid impedance, faults, and feedback delays. Park's transformation provides accurate control over reactive and active (real) power. This enhances the overall efficiency of the system by enabling operators to control reactive power compensation and optimize energy flow. In dynamic settings, this guarantees greater system stability and faster response times. The current paper aims to improve the grid system by utilizing the dq0 controller. The current work focuses on the analysis based on simulations and theory, where the state space equation serves as the basis for dq-axis current decoupling. A MATLAB platform was used to simulate the complete system. TDH values of 2.45%, or less than 5%, in the given results are acceptable. The suggested controller was hence appropriate for grid system applications.

Keywords

Grid System, Inverter, Optimization, Energy, Three Phase

1. Introduction

In many areas, including elevator energy feedback, the three-phase grid-connected inverter is the key to energy-saving technology [1]. In this way, the excess DC energy can be converted to AC and connected to the power grid, which acts as the load. The advantages of the three-phase voltage type inverter lower alternating current side harmonic current, two-way energy flow, and higher power factor make it a popular choice for three phase grid-connected control systems [2]. employs the inverse compensation and superposition principle to achieve current decoupling in a three-phase static coordinate system; subsequently, the hysteresis comparison output is used to control the inverter switch to achieve current tracking [3]. The drawback of this approach is that the switching frequency is not fixed, making it challenging to design the output filter [4]. Previous works have mentioned the use of auto-disturbance rejection power algorithm and feedback linearization in dq coordinate systems; reference [5] also addresses dq coordinate system using a combination of composite vector and predictive current control, but the decoupling process was too complex. uses a PR decoupling control method, [6] uses a non-delay beat current predictive control method. Furthermore, the procedure of implementation is very complicated, which makes it difficult for practical application [7]. A theoretical approach to current decoupling has been proven in reference [8], with good simulation results achieved. However, the process of demonstration is complicated and does not provide an explanation of how compensation parameters can be adjusted in theory. A novel approach, known as split current decoupling, is presented in reference [9]. However, there is no concrete theoretical proof, the splitting weight parameter is highly unpredictable, and it is hard to determine. The majority of the aforementioned materials simply provide theoretical analysis and simulation; they do not provide information on the actual application procedure or the outcomes of experimental verification. More research is required to determine whether the complicated theory's practical implementation is feasible. However, from the above paper, we can infer that, to date, the researchers have not implemented a dq controller in the three-phase grid that is suitable for three phase grid system control. Most notably, by converting the three-phase abc-reference frame into the dqo-coordinate system, the dqo-coordinate system offers a notable improvement in inverter/motor control. The primary objective of the current study is to simplify the analysis of a three-phase grid-connected system using Park's transformation. For easier analysis of unbalanced and distorted waveforms, making it a valuable tool in power system studies. The use of Park's transformation process in a three-phase grid-connected system is what makes the current work novel. Because of this simplification, control systems operate more accurately and efficiently. This research examines in detail a three-phase grid-connected inverter control system that is based on the orientation of the grid voltage. Theoretical analysis, simulation analysis. The dq-axis current decoupling concept is derived from the state space equation. The limitations associated with fossil fuels have progressively prompted the creation of alternate energy sources, specifically renewable energy sources [10]. The way photovoltaic systems are connected to the grid has changed recently in response to the need for specific electrical charges that can only be supplied by alternate voltage as well as the rise in the usage of clean, carbon-free energy [11]. Systems that are connected to the grid are crucial to the generation of distributed energy.

Their use is expanding throughout the community with the support of government incentives [12]. These systems are made up of an inverter that changes direct current into alternating current and a photovoltaic generator that converts solar energy into direct current. There are two types of PV inverters on the market: single-phase and three-phase, with reference to grid connection [13]. Chain converters with a power output between 1 and 5 kW are commonly employed in low-power solar systems that are linked to the home and medium power grid. The majority of inverter topologies are three-phase when the output range is more than 10 kW [14]. Because three-phase topologies do not have an electrolyte capacitor and do not place as much stress on semiconductors and magnetic components during dimensioning, they are more cost-effective, smaller in size, and have a longer service life than single-phase inverters [15]. Will examine the different three-phase inverter topologies and their benefits and drawbacks. It is anticipated that the solar industry's growth would result in a spike in demand for grid connections, requiring the extension and renovation of the current infrastructure [16]. Resources may be strained; therefore, cautious planning is needed [11]. The grid-connected systems that have been implemented up to this point face various issues despite using distinct control techniques. Simplified approval procedures, upgraded grid infrastructure, grid connection for renewable energy projects priority, distributed energy resources (DERs) and microgrid integration, enhanced coordination and communication, legislative changes, and incentives are some of these. Voltage, frequency, and harmonic fluctuations can provide problems for systems that are freestanding or grid-connected. The power supply's functionality and stability may be impacted by several problems [17]. DQ controllers provide accurate control over reactive and active (real) power. This enhances the overall efficiency of the system by enabling operators to control reactive power compensation and optimize energy flow [18]. Reactive power averaging is not necessary with DQ controllers, allowing for instantaneous adjustment. In dynamic settings, this guarantees greater system stability and faster response times [19].

The rest of this paper is organized as follows: A mathematical representation of a three-phase grid connector is presented in Section 2. Results and discussions were carried out in Section 3, and conclusions were drawn in Section 4.

2. Mathematical Models of the Three-Phase Grid Connector System

Figure 1 depicts the primary circuit of the three-phase grid-connected inverter. Consequently, as illustrated in **Figure 1**, the current of the parallel grid is defined as the positive the direction from a positive charge to a lesser charge, or a negative charge, or a negative charge to an even more negative charge. The phase inductance is L, while the equivalent resistance of the filter inductor is R. When the grid voltage exhibits three phase symmetry, the three-phase circuit remains independent of one another, and the output voltage of the inverter bridge is thereby ignoring the high-frequency component. (1) displays the mathematical representation of a three-phase grid-connected inverter in the ABC coordinate system. A grid-connected inverter's control method simplifies the inverter's control by converting the three-phase AC quantities into a two-phase DC reference frame. It simplifies the inverter's control by converting the three-phase AC quantities into a two-phase DC reference frame. The three-phase AC currents and voltages are transformed into two DC components, d and q, by the DQ controller using the dq-transformation. The active and reactive power flows are represented by these elements, respectively. After that, the controller adjusts these parts to produce the required power output and synchronize the grid. A simple Phase-Locked Loop (PLL) that is used to retrieve the phase information of three-phase voltages is the DQ-type PLL. In a rotating frame reference, it works by minimizing the voltage projected on the quadrature axis.

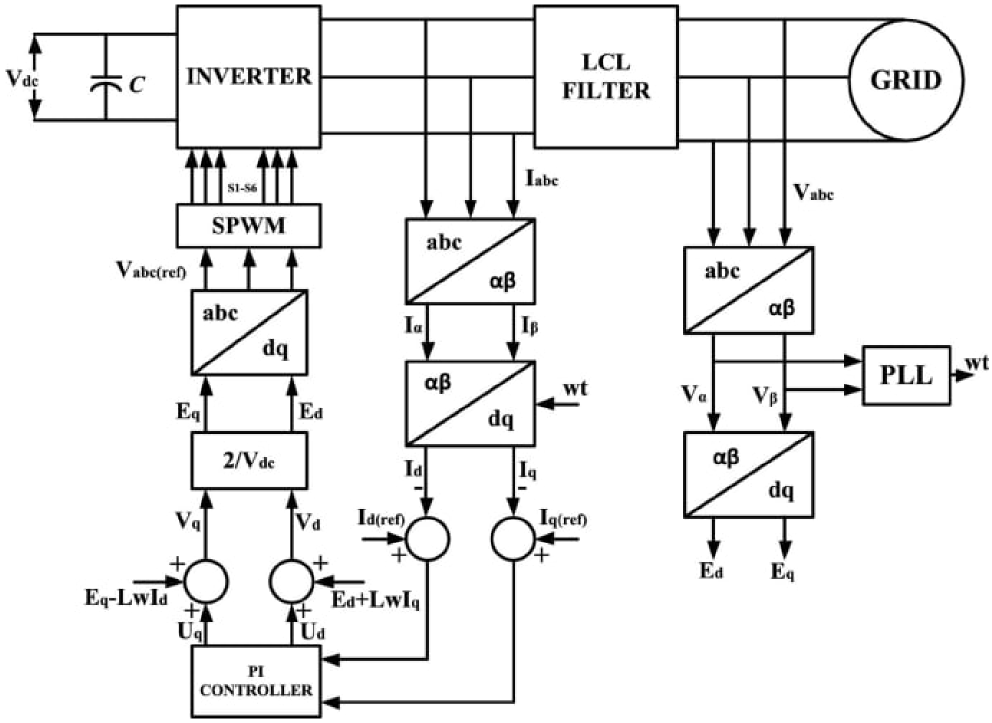

Figure 1. Using the dq axis, control a three-phase grid-connected inverter [16].

A grid-connected inverter's control method. It simplifies the inverter's control by converting the three-phase AC quantities into a two-phase DC reference frame. The three-phase AC currents and voltages are transformed into two DC components, d and q, by the DQ controller using the dq-transformation. The active and reactive power flows are represented by these elements, respectively. After that, the controller adjusts these parts to produce the required power output and synchronize the grid. A simple Phase-Locked Loop (PLL) that is used to retrieve the phase information of three-phase voltages is the DQ-type PLL. In a rotating frame reference, it works by minimizing the voltage projected on the quadrature axis.

$$\begin{bmatrix} L\frac{d_{Ia}}{dt} \\ L\frac{d_{Ib}}{dt} \\ L\frac{d_{Ic}}{dt} \end{bmatrix} = \begin{bmatrix} -R & 0 & 0 \\ 0 & -R & 0 \\ 0 & 0 & -R \end{bmatrix} \begin{bmatrix} i_a \\ i_b \\ i_c \end{bmatrix} - \begin{bmatrix} 1 & 0 & 0 \\ 0 & 1 & 0 \\ 0 & 0 & 1 \end{bmatrix} \begin{bmatrix} V_a \\ V_b \\ V_c \end{bmatrix} + \begin{bmatrix} 1 & 0 & 0 \\ 0 & 1 & 0 \\ 0 & 0 & 1 \end{bmatrix} \begin{bmatrix} e_a \\ e_b \\ e_c \end{bmatrix} \tag{1}$$

The physical values in static coordinates can be changed into physical quantities in the two-phase synchronous rotating dq coordinate system by using coordinate transformation, as demonstrated in (2).

$$\begin{bmatrix} \frac{Ld_{id}}{dt} \\ \frac{Ld_{iq}}{dt} \end{bmatrix} = \begin{bmatrix} -R & wL \\ wL & -R \end{bmatrix} \begin{bmatrix} i_d \\ i_q \end{bmatrix} - \begin{bmatrix} 1 & 0 \\ 0 & 1 \end{bmatrix} \begin{bmatrix} V_d \\ V_q \end{bmatrix} + \begin{bmatrix} 1 & 0 \\ 0 & 1 \end{bmatrix} \begin{bmatrix} e_d \\ e_q \end{bmatrix} \tag{2}$$

Put (2) in the equation's form and slightly alter it as (3) indicates.

$$\begin{cases} \frac{Ld_{id}}{dt} + i_d R = V_d + \omega L_{iq} - e_d \\ \frac{Ld_{iq}}{dt} + i_q R = V_q + \omega L_{id} - e_q \end{cases} \tag{3}$$

(3) illustrates how challenging it is to construct a current controller due to the coupling of the current between the d- and q-axes. Nevertheless, a thorough analysis reveals that the variable quantity of the d- or q-axis current is located at the left end of the equation. Consequently, the left-hand expression of the preceding equation can be substituted with the closed-loop PI regulator to obtain zero steady-state error, as indicated by the following (4).

$$\begin{cases} K_{pd}\left(1+\frac{1}{\tau_{id}S}\right) = v_d + \omega L_{iq} - e_d \\ K_{pd}\left(1+\frac{1}{\tau_{id}S}\right) = v_q - \omega L_{id} - e_q \end{cases} \tag{4}$$

By further deforming (4), it is possible to acquire the output voltages v_d and v_q as indicated in (5).

$$\begin{cases} V_d = K_{pd}\left(1+\frac{1}{\tau_{id}S}\right) - \omega L_{iq} + e_d \\ V_q = K_{pd}\left(1+\frac{1}{\tau_{iq}S}\right) + \omega L_{id} + e_q \end{cases} \tag{5}$$

The current of the d axis is direct current d i_d in (5), and the current of the q axis is $i_q \sim 0$. if the d axis of the dq axis is oriented in the direction of the grid voltage vector. Simultaneously, the easiest way allows the coupling ωL_{iq} to be removed directly for the d axis.

It is possible to think of the disturbance of the grid voltage d e as a disturbance of the power network voltage, and the disturbance can be eliminated by using feed-forward control. For the q axis, the same holds true. As a result, the control system's dq axis decoupling is achieved based on (5).

The traditional voltage-source inverter, operating in three phases, has six power transistors. There are eight operational states. Eight voltage vectors, of which six fundamental vector modes have lengths equal to $\frac{2}{3V_{dc}}$, correspond to the inverter. Two additional states are associated with (000) and (111). By using the corresponding reference vector of these eight fundamental space vectors, space vector modulation (SVPWM) approximates the ideal circle in a relatively short amount of time for the vector trajectory of three phase grid-connected current. Using the first sector as an example, Figure 2 illustrates how two adjacent basic voltage vectors V_1, V_2 and zero vector V_0 are employed to create reference vectors V_{ref}, and using the volt-second balance principle, the following formula can be found.

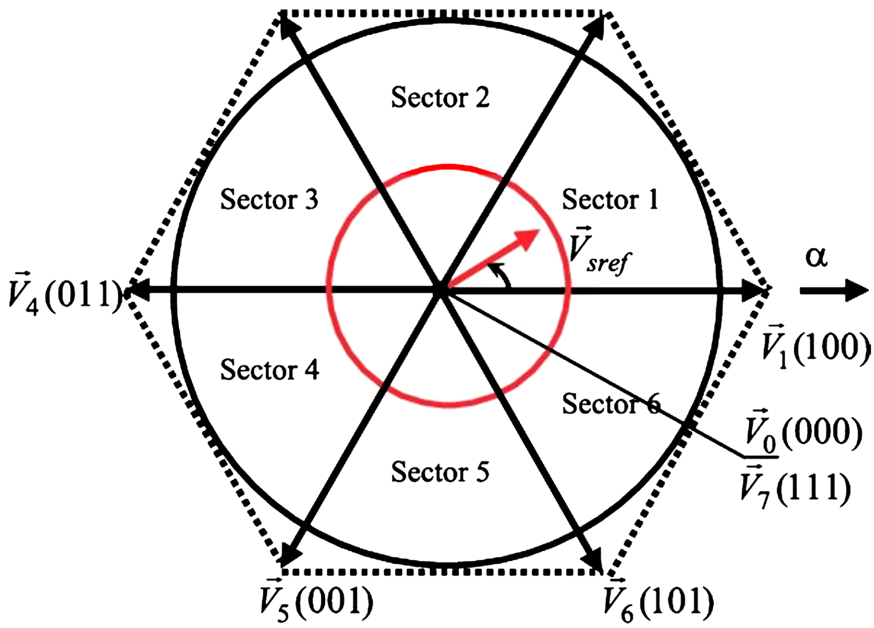

Figure 2. Basic space voltage vector and sectors [18].

$$T_1V_1 + T_2V_2 + T_0V_0 = T_sV_{ref} \tag{6}$$

Formula (7) can be used to get the action time in the following way:

$$\begin{cases} T_1 = \dfrac{T_s}{2V_{dc}}\left(3V_{\propto} - \sqrt{3V_{\beta}}\right) \\ T_2 = \dfrac{\sqrt{3}T_s}{V_{dc}} - V_{\beta} \\ T_0 = T_s - T_1 - T_2 \end{cases} \tag{7}$$

Phase-locking is achieved by sampling the three-phase grid voltage using the reactive current control approach. As indicated in (8), the tracking phase angle and frequency of the grid-connected current are used to determine the phase and frequency signals of the grid voltage.

$$\theta_e = \tan\left(\frac{e_\beta}{e_\alpha}\right) \tag{8}$$

Following the sampling of the three-phase grid-connected current, the supplied grid-connected current reference is used to perform PI regulation after the Q-axis current and Q-axis current are obtained via coordinate transformation. The aforementioned power network voltage feed forward control and decoupling regulate the outcomes. Next, the $\frac{dq}{\alpha\beta}$ transform can be used to obtain V_α and V_β. Ultimately, the unit power factor is connected to the grid and the power bridge switch is driven by the duty cycle signal via the SVPWM module.

For a sine PWM modulation scheme, the relation between modulation index and inverter voltage is given by

$$\begin{cases} V_d = m_d * \left(\frac{V_{dc}}{2}\right) \\ V_q = m_q * \left(\frac{V_{dc}}{2}\right) \end{cases} \tag{9}$$

After obtaining mathematical models, we used for the simulation a 100 kVA, three-phase grid inverter with an 800-volt DC input and a 10-kilo hertz switching frequency.

In order to apply the dq_0 controller, the basic assumptions for the park's transformation are used in this work. These are

Case 1: The q-axis is leading the d-axis by 90 electrical degrees; and the angle between the d-axis with respect to the a-axis is used.

$$\begin{cases} \left[f_{dq0}\right] = \left[T_{dq0}\left(\theta_d\right)\right]\left[f_{abc}\right] \\ \left[f_{dq0}\right] = \begin{bmatrix} f_d \\ f_q \\ f_0 \end{bmatrix} \\ \left[f_{abc}\right] = \begin{bmatrix} f_a \\ f_b \\ f_c \end{bmatrix} \end{cases} \tag{10}$$

and

$$\left[T_{dq0}\left(\theta_d\right)\right] = \frac{2}{3}\begin{bmatrix} \cos\theta_d & \cos\left(\theta_d - \frac{2\pi}{3}\right) & \cos\left(\theta_d + \frac{2\pi}{3}\right) \\ -\sin\theta_d & -\sin\left(\theta_d - \frac{2\pi}{3}\right) & -\sin\left(\theta_d + \frac{2\pi}{3}\right) \\ \frac{1}{2} & \frac{1}{2} & \frac{1}{2} \end{bmatrix} \tag{11}$$

Case 2: The q-axis is lagging the d-axis by 90 electrical degrees; and the angle between the d-axis with respect to the a-axis is used.

$$\begin{cases} \left[f_{abc}\right] = \left[T_{dq0}\left(\theta_d\right)\right]^{-1}\left[f_{dq0}\right] \\ \left[f_{dq0}\right] = \begin{bmatrix} f_d \\ f_q \\ f_0 \end{bmatrix} \\ \left[f_{abc}\right] = \begin{bmatrix} f_a \\ f_b \\ f_c \end{bmatrix} \end{cases} \tag{12}$$

$$\left[T_{dq0}\left(\theta_d\right)\right]^{-1} = \begin{bmatrix} \cos\theta_d & \sin\theta_d & 1 \\ \cos\left(\theta_d - \frac{2\pi}{3}\right) & \sin\left(\theta_d - \frac{2\pi}{3}\right) & 1 \\ \cos\left(\theta_d + \frac{2\pi}{3}\right) & \sin\left(\theta_d + \frac{2\pi}{3}\right) & 1 \end{bmatrix} \tag{13}$$

Case 3: The q-axis is leading the d-axis by 90 electrical degrees, and the angle between the q-axis with respect to the a-axis is used.

$$\left[T_{qd0}\left(\theta_q\right)\right]^{-1} = \begin{bmatrix} \cos\theta_q & \sin\theta_q & 1 \\ \cos\left(\theta_q - \frac{2\pi}{3}\right) & \sin\left(\theta_q - \frac{2\pi}{3}\right) & 1 \\ \cos\left(\theta_q + \frac{2\pi}{3}\right) & \sin\left(\theta_q + \frac{2\pi}{3}\right) & 1 \end{bmatrix} \tag{14}$$

where

$$\begin{cases} \theta_q = \theta_d + \theta_0 \\ \theta_q = \theta_d + \frac{\pi}{2} \\ \theta_d = \omega t + \theta_0 \end{cases} \tag{15}$$

3. Results and Discussion

Figure 3 shows simulated results for the three-phase grid connector. Three-phase voltage and three-phase currents were displayed. The green line indicates phase A, whereas the yellow line implies phase B. Phase C was demonstrated in the red line. All lines are oscillated between −600 V and 600 V. This means a bounded sinusoidal function is a type of function that oscillates between two defined limits, unlike a regular sine wave that extends infinitely in both directions. This property makes it useful in various applications, such as grid processing and control systems. Meanwhile, currents are different in magnitude. Phase C current is bounded between nearly −10 A and 200 A, and phase B current is between −100 A and 10 A. Phase A current is −200 A to 0 A. Nearly phase C into the phase with its voltage, whereas phase A and phase B are out of the phase. In this work environment, the voltage and current waveforms attain their maximum and minimum values simultaneously. Conversely, out of phase indicates that, depending on the parts of the circuit, the current peaks either before or after the voltage peaks. It's not always the case that a negative current value indicates a mistake. It just indicates that the true direction of travel is different from the first assumption. A number of things, including measurement setup, component behavior, and circuit configuration, may cause this. The specific shape and characteristics of the voltage waveform provide information about the nature of the electrical signal, such as its frequency, amplitude, and voltage levels. Analyzing the voltage waveform is essential in various electrical and electronic applications, including circuit design, signal analysis, and troubleshooting. The engineering meanings of the voltage waveforms in Figure 3 could be interpreted as the voltage variation over time. It shows the changes in the voltage level of an electrical signal or circuit. A smooth, continuous wave that represents a sinusoidal voltage variation. Meanwhile, analyzing the current waveform can provide valuable information about the operating conditions, efficiency, and potential issues in an electrical circuit or system. It is an important tool for electrical engineers and technicians when investigating, troubleshooting, and designing various electronic devices and circuits. The frequency of a current is how many times one cycle of the waveform is repeated per second and is measured in hertz (Hz). Current can be generated as an alternating current (AC), where the direction of the current flow alternates around zero with positive and negative directions (bipolar; Figure 3). This is a smooth, wave-like pattern that rises and falls in a sinusoidal curve. This is typical in AC (alternating current) circuits. The variation of electric current over time. It shows the magnitude and direction of the current as it changes within a given time period. The current waveform can take different shapes or patterns depending on the type of electrical circuit and the components involved. PQ event or events may be present in the voltage waveform, which is expected to be a periodic (sinusoidal) waveform. The initial stage of pre-processing involves separating the non-stationary component from the voltage waveform. There is a transient portion and an event-related part to the non-stationary section. This specific event-related portion of the waveform is subjected to additional analysis, most often consisting of feature extraction using signal processing methods. Typically, the disturbance portion is separated and the distorted signal (RMS value) is compared to the matching pure signals. Two categories of techniques are frequently suggested for signal segmentation. These techniques range from non-parametric to parametric. In parametric approaches, such as the Kalman filter method and auto-regressive models, a portion of the waveform is fitted to the selected model, yielding notable residuals. Non-parametric techniques include the PQ signal's multi-state decomposition and the extraction of singular points using the Fourier transform (FT/STFT) and wavelet transform (WT). When the voltage and current waveforms are analyzed simultaneously, as in Figure 3, it is evident that the current is at its peak or maximum when the voltage is. As the instantaneous voltage drops in value, there is a decrease in the current flow. The current is 0 when the voltage is zero. Observe that the direction of the current flow is dictated by the voltage's polarity. In other words, in the above example, a positive 10 amperes flow at a voltage of 10 volts, and a negative 10 amperes flows at a value of 10 volts.

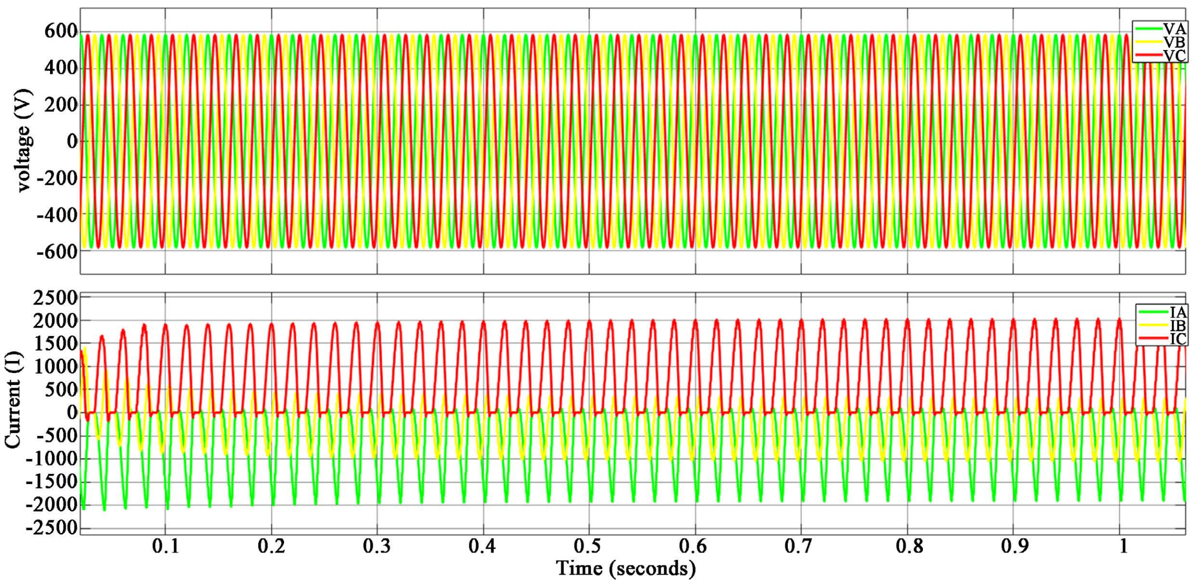

Figure 3. Three phase line.

Figure 4 demonstrated hysteresis loss. Hysteresis loss, or energy loss, occurs in grid-connected systems due to magnetic materials (capacitors and inductors) being subjected to a changing magnetic field. This loss is caused by the friction between the magnetic domains within the material as they try to align with the changing field (**Figure 4**). The blue line indicates the path of the hysteresis loss, and the red dot on the hysteresis loss indicates the animated profile. The loss in magnetic flux per unit was represented vertically, whereas the horizontal axis represented currents per unit. Coercive current was ±0.004 pu. The TDH loss was 2.45%, which is less than 5% and acceptable. Because ferromagnetic material is involved, hysteresis loss is a manifestation of the phenomena of hysteresis. When the external field is eliminated, some of the magnetic field's energy is not transferred back into the circuit in ferromagnetic materials. A hysteresis loop illustrates the relationship between the magnetizing force (H) and the induced magnetic flux density (B), illustrating how ferromagnetic materials lose heat in an AMF because of hysteresis loss. When MNPs are exposed to an external field, magnetization demonstrates that the magnetic moment begins to align in the direction of the field, a phenomenon that typically only happens at large field magnitudes. As illustrated in **Figure 4**, in order to cause the particles' magnetization to flip, hysteresis must be overcome. This causes the particles to heat up when an alternating field is provided with an amplitude at least twice that of the particles' coercivity. The MNPs continue to emit heat in proportion to the area of their hysteresis loop. The hysteresis loss heat emitted by the ferromagnetic material is reported. The energy dissipated in a magnetic material or an electrical component due to the phenomenon of hysteresis. Hysteresis is the lagging of the magnetization of a material behind the changes in the applied magnetic field. In electrical grid systems, hysteresis loss can occur in transformer cores, electric motors, generators, and other electromagnetic components. This energy loss is caused by the repeated changing of the magnetic fields within these components as the alternating current (AC) flows through them. Hysteresis loss reduces the overall efficiency of the electrical grid system, as it represents energy that is dissipated as heat rather than being used for useful work. Minimizing hysteresis losses is an important consideration in the design and operation of electrical grid components to improve the overall efficiency of the system. Hysteresis means that the output of the circuit changes with a border. Example: If the input rises from 0 to 3 V, the output changes to 0 V. If the input lowers from 3 V to 2 V, the output changes to 5 V. We have a hysteresis of 1 V while loop between 2.1 V and 2.9 V, and the output will not be changing.

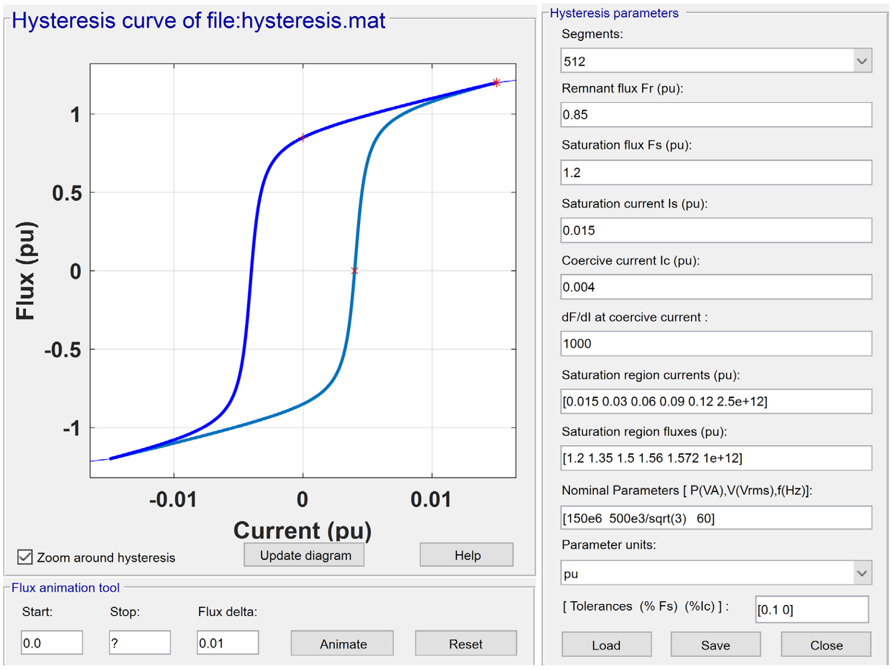

Figure 4. Hysteresis loss for three phase grid connectors.

Table 1 shows the obtained results for the phase-to-phase voltage. Even though all the phase-to-phase voltages were the same (386.9 V), the angles were different (90, −150, −30, −60, 60, 180) for the VAB, VBC, and VCA, respectively. The negative values of the angle indicate the phase voltages and phase currents are out of phase, whereas the positive values of the angle tell us the phase voltages and phase currents are in phase.

Table 2 shows the comparison of existing results with the current work. Accordingly, phase-to-phase voltages of current work are 34.3% improved over existing works, whereas phase-to-phase currents are 89.7% improved over existing work. From these results, we can infer that Park's transformation converts three-phase AC quantities into a rotating reference frame (dq), simplifying control algorithms. This improves the efficiency and accuracy of control systems. Park's Transformation facilitates the analysis of harmonics in power systems. It helps identify and mitigate harmonic distortion, improving power quality.

Table 3 showed the computations of different frequency dependent parameters.

Table 1. Measurements and state analyzer.

Types of measurements:	Obtained results	Obtained angle (˚)
VAB	386.9 V	90
VBC	386.9 V	−150
VCA	386.9 V	−30
IAB	0.006811 A	−60
IBC	0.006811 A	60
ICA	0.006811 A	180

Table 2. Analysis of measurement comparisons.

Types of measurements:	Obtained results of current work	Results of existing work [20]	Improvement (%)
VAB	386.9 V	589 V	34.3%
VBC	386.9 V	589 V	34.3%
VCA	386.9 V	589 V	34.3%
IAB	0.006811 A	0.066	89.7%
IBC	0.006811 A	0.066	89.7%
ICA	0.006811 A	0.066	89.7%

Table 3. Computed frequency dependent variables parameters.

Types of the parameters	Obtained results
$R_{\text{matrix}}\left(\frac{\text{ohm}}{\text{km}}\right)$	$\begin{bmatrix} 0.1071 & 0.09729 & 0.09499 \\ 0.09729 & 0.1105 & 0.09729 \\ 0.09499 & 0.09729 & 0.1071 \end{bmatrix}$
$L_{\text{matrix}}\left(\frac{\text{H}}{\text{km}}\right)$	$\begin{bmatrix} 0.00158 & 0.00075 & 0.00062 \\ 0.00075 & 0.00157 & 0.00075 \\ 0.00062 & 0.00075 & 0.00158 \end{bmatrix}$
$C_{\text{matrix}}\left(\frac{\text{H}}{\text{km}}\right)$	$\begin{bmatrix} 1.16613\times10^{-8} & -2.12683\times10^{-9} & -5.83623\times10^{-10} \\ -2.12683\times10^{-9} & 1.21174\times10^{-8} & -2.12683\times10^{-9} \\ -5.83623\times10^{-10} & -2.12683\times10^{-9} & 1.16613\times10^{-8} \end{bmatrix}$
Positive and zero-sequence parameters at 50 Hz	$\begin{bmatrix} [R_1, R_0]\left(\frac{\text{ohm}}{\text{km}}\right) = [0.01171 \quad 0.30127] \\ [L_1, L_0]\left(\frac{\text{H}}{\text{km}}\right) = [0.00087 \quad 0.00299] \\ [C_1, C_0]\left(\frac{\text{F}}{\text{km}}\right) = [1.34257\times10^{-8} \quad 8.58845\times10^{-9}] \end{bmatrix}$

4. Conclusions

In this paper, we design the mathematical models for three phase grid connector system. The dq_0 controllers were proposed, and formulated. Every line oscillates between 600 and −600 volts. This means that, in contrast to a standard sine wave, which extends infinitely in both directions, a bounded sinusoidal function oscillates between two defined limits. Because of this feature, it can be applied to a variety of tasks, including control systems and grid processing. Currents vary in magnitude in the meantime. Phase B current is limited between −100 A and 10 A, whereas phase C current is confined between about −10 A and 200 A. −200 A to 0 A is the phase A current. The horizontal axis showed currents per unit, whereas the vertical axis showed the loss in magnetic flux per unit. Information about the frequency, amplitude, and voltage levels of the electrical signal can be inferred from the particular shape and properties of the voltage waveform. In many electrical and electronic applications, such as circuit design, signal analysis, and troubleshooting, analyzing the voltage waveform is crucial. One possible interpretation of the voltage waveforms' engineering connotations is the voltage variation over time. It displays variations in an electrical signal's or circuit's voltage level. a continuous, smooth wave that symbolizes a sinusoidal voltage fluctuation. In the meantime, examining the current waveform might reveal important details regarding the efficiency, possible problems, and working conditions of an electrical circuit or system. When researching, debugging, and building different electronic devices and circuits, it is a crucial tool for electrical engineers and technicians. A current's frequency, expressed in hertz (Hz), is the number of times a waveform's cycle is repeated every second. Alternating current (AC) is a form of current generation in which the flow of current alternates between positive and negative directions with relation to zero (bipolar). This pattern has a sinusoidal rise and fall rhythm and is smooth and wave-like. Circuits with alternating current (AC) often operate like this. The change in electric current over a certain duration. It displays the current's direction and magnitude as it varies over a specified amount of time. Depending on the kind of electrical circuit and the components used, the current waveform can assume various forms or patterns. The expected periodic (sinusoidal) waveform of the voltage may contain one or more PQ events. Removing the non-stationary component from the voltage waveform is the first step in the pre-processing procedure. The non-stationary component consists of an event-related portion and a transient portion. Further analysis, usually in the form of feature extraction via signal processing techniques, is applied to this particular event-related section of the waveform. Usually, after separating the disturbance component, the distorted signal (RMS value) is contrasted with the pure signals that match. Typically, two types of methods are recommended for signal segmentation. These methods span the spectrum from parametric to non-parametric. Part of the waveform is fitted to the chosen model in parametric approaches, such as the Kalman filter method and auto-regressive models, producing significant residuals. Non-parametric methods include the multi-state decomposition of the PQ signal and the Fourier transform (FT/STFT) and wavelet transform (WT) for the extraction of singular points. The link between the induced magnetic flux density (B) and the magnetizing force (H) is shown by a hysteresis loop, which shows how ferromagnetic materials lose heat in an AMF due to hysteresis loss. Magnetization shows that when MNPs are subjected to an external field, the magnetic moment starts to align with the field, a phenomenon that usually occurs only at large field magnitudes. Hysteresis needs to be overcome for the particles' magnetization to flip. When an alternating field is applied that is at least twice as strong as the particles' coercivity, this results in the particles heating up. According to the size of their hysteresis loop, the MNPs keep emitting heat. The heat released by the ferromagnetic material during hysteresis loss is recorded. The energy is lost as a result of the hysteresis phenomena in an electrical component or magnetic substance. The phenomenon known as hysteresis occurs when a material's magnetization lags behind variations in the applied magnetic field. Transformer cores, electric motors, generators, and other electromagnetic components in electrical grid systems are susceptible to hysteresis loss. The alternating current (AC) passing through these components causes the magnetic fields inside of them to repeatedly change, which results in energy loss. Because hysteresis loss is energy that is lost as heat instead of being put to good use, it lowers the overall efficiency of the electrical grid system.

In order to increase system efficiency overall, minimizing hysteresis losses is a crucial factor in the design and operation of electrical grid components. Hysteresis is the result of a border-like change in the circuit's output. Current under coercion was ±0.004 pu. With a TDH loss of 2.45%, it is reasonable and less than 5%. Therefore, the proposed controllers were suitable for controlling three phase grid connector system.

Acknowledgments

The authors thank, and acknowledge Sairoel Amertet (Dr. Engineering) for his expertise and assistance throughout all aspects of our study and for their help in writing the manuscript.

Conflicts of Interest

The authors declare no conflicts of interest regarding the publication of this paper.

References

[1] Yao, Z., Xiao, L. and Guerrero, J.M. (2015) Improved Control Strategy for the Three-Phase Grid-Connected Inverter. *IET Renewable Power Generation*, **9**, 587-592. https://doi.org/10.1049/iet-rpg.2014.0350

[2] Subsingha, W. (2016) Design and Analysis Three Phase Three Level Diode-Clamped Grid Connected Inverter. *Energy Procedia*, **89**, 130-136. https://doi.org/10.1016/j.egypro.2016.05.019

[3] Guerrero-Rodríguez, N.F., Rey-Boué, A.B. and Reyes-Archundia, E. (2017) Overview and Comparative Study of Two Control Strategies Used in 3-Phase Grid-Connected Inverters for Renewable Systems. *Renewable Energy Focus*, **19**, 75-89. https://doi.org/10.1016/j.ref.2017.05.007

[4] Mechouma, R., Azoui, B. and Chaabane, M. (2012) Three-Phase Grid Connected Inverter for Photovoltaic Systems, a Review. 2012 *First International Conference on Renewable Energies and Vehicular Technology*, Nabeul, 26-28 March 2012, 37-42. https://doi.org/10.1109/revet.2012.6195245

[5] Chen, Y. and Smedley, K. (2008) Three-Phase Boost-Type Grid-Connected Inverter. *IEEE Transactions on Power Electronics*, **23**, 2301-2309. https://doi.org/10.1109/tpel.2008.2003025

[6] Liu, F., Zha, X., Zhou, Y. and Duan, S. (2009) Design and Research on Parameter of LCL Filter in Three-Phase Grid-Connected Inverter. 2009 *IEEE 6th International Power Electronics and Motion Control Conference*, Wuhan, 17-20 May 2009, 2174-2177. https://doi.org/10.1109/ipemc.2009.5157762

[7] Li, R., Ma, Z. and Xu, D. (2012) A ZVS Grid-Connected Three-Phase Inverter. *IEEE Transactions on Power Electronics*, **27**, 3595-3604. https://doi.org/10.1109/tpel.2012.2184559

[8] Nandurkar, M.S.R. and Rajeev, M.M. (2012) Design and Simulation of Three Phase Inverter for Grid Connected Photovoltic Systems. *Proceedings of Third Biennial National Conference*, *NCNTE*-2012, 24-25 February 2012, 80-83.

[9] Hintz, A., Prasanna, U.R. and Rajashekara, K. (2016) Comparative Study of the Three-Phase Grid-Connected Inverter Sharing Unbalanced Three-Phase and/or Single-Phase Systems. *IEEE Transactions on Industry Applications*, **52**, 5156-5164. https://doi.org/10.1109/tia.2016.2593680

[10] Yu, J., Lin, X., Song, D., Yu, R., Yang, J. and Su, M. (2020) New Perspectives on Stability Analysis of Three-Phase Grid-Connected Inverter Considering System Couplings. *IEEE Transactions on Power Systems*, **35**, 1967-1978. https://doi.org/10.1109/tpwrs.2019.2957393

[11] Liu, A., Hou, C., Zhu, M., Wen, Y. and Cai, Y. (2024) DC-Link Power Ripple Mitigation of Three-Phase Grid-Tied Inverters with Virtual Phase-Current Regulation. *IEEE Transactions on Industrial Electronics*, 1-12. https://doi.org/10.1109/tie.2024.3360617

[12] Geng, H., Xu, Y. and Wu, W. (2024) Aliasing Suppression Method for a Three-Phase Grid-Connected Photovoltaic Inverter Based on Multi-Sampling and Mean Filtering. *Energies*, **17**, Article 907. https://doi.org/10.3390/en17040907

[13] Ouai, A., Mokrani, L., Machmoum, M. and Houari, A. (2024) Voltage Error Estimation-Based Fault Diagnosis Method for Three-Phase PWM-Inverter in Grid-Connected Photovoltaic Power System without Any Over-Rating. *Periodica Polytechnica Electrical Engineering and Computer Science*. https://doi.org/10.3311/ppee.23416

[14] Khan, L., Khan, L., Agha, S., Hafeez, K. and Iqbal, J. (2024) Passivity-Based Rieman Liouville Fractional Order Sliding Mode Control of Three Phase Inverter in a Grid-Connected Photovoltaic System. *PLOS ONE*, **19**, e0296797. https://doi.org/10.1371/journal.pone.0296797

[15] Abu-Zaher, M., Zhuo, F., Orabi, M., Hassan, A. and Gaafar, M.A. (2024) Dual-Input Configuration of Three-Phase Split-Source Inverter for Photovoltaic Systems with Independent Maximum Power Point Tracking. *Electric Power Systems Research*, **232**, Article 110375. https://doi.org/10.1016/j.epsr.2024.110375

[16] Boutaghane, K., Bennecib, N., Benidir, M., Benbouhenni, H. and Colak, I. (2024) Performance Enhancement of a Three-Phase Grid-Connected PV Inverter System Using Fractional-Order Integral Sliding Mode Controls. *Energy Reports*, **11**, 3976-3994. https://doi.org/10.1016/j.egyr.2024.03.049

[17] Baltacı, K., Ertekin, D. and Bayrak, G. (2024) Design and Experimental Validation of an Artificial Neural Network-SVPWM Controller for a Novel Micro Grid-Tied Fuel Cell-Based 3-Phase Boost Inverter. *International Journal of Hydrogen Energy*, **52**, 1247-1265. https://doi.org/10.1016/j.ijhydene.2023.10.291

[18] Khan, M.Z., Haque, A., Malik, A., Amir, M., Zahgeer, F.S. and Khalid, H.M. (2024) A Critical Review on Control Techniques for Parallel Operated Inverters in Grid Connected and Standalone Mode. 2024 *International Conference on Green Energy, Computing and Sustainable Technology* (*GECOST*), Miri Sarawak, 17-19 January 2024, 66-71. https://doi.org/10.1109/gecost60902.2024.10475094

[19] He, Y., Li, Y., Zhou, B. and Peng, F.Z. (2024) Switching-Cycle-Based Startup for Grid-Connected Inverters. *IEEE Journal of Emerging and Selected Topics in Industrial Electronics*, 1-12. https://doi.org/10.1109/jestie.2024.3365031

[20] Lin, X., Liu, Y., Yu, J., Yu, R., Zhang, J. and Wen, H. (2022) Stability Analysis of Three-Phase Grid-Connected Inverter under the Weak Grids with Asymmetrical Grid Impedance by LTP Theory in Time Domain. *International Journal of Electrical Power & Energy Systems*, **142**, Article 108244. https://doi.org/10.1016/j.ijepes.2022.108244